[Downloaded from www.aece.ro on Saturday, October 13, 2018 at 09:10:47 (UTC) by 159.226.100.198. Redistribution subject to AECE license or copyright.]

FPA Tuned Fuzzy Logic Controlled Synchronous Buck Converter for a Wave/SC Energy System

Erdinc SAHIN[1], Ismail Hakki ALTAS[2]
[1]*Surmene Abdullah Kanca VHS, Karadeniz Technical University, Trabzon, 61530, Turkey*
[2]*Department of Electrical and Electronics Engineering, Karadeniz Technical University, Trabzon, 61080, Turkey*
esahin@ktu.edu.tr

***Abstract*—This paper presents a flower pollination algorithm (FPA) tuned fuzzy logic controlled (FLC) synchronous buck converter (SBC) for an integrated wave/ supercapacitor (SC) hybrid energy system. In order to compensate the irregular wave effects on electrical side of the wave energy converter (WEC), a SC unit charged by solar panels is connected in parallel to the WEC system and a SBC is controlled to provide more reliable and stable voltage to the DC load. In order to test the performance of the designed FLC, a classical proportional-integral-derivative (PID) controller is also employed. Both of the controllers are optimized by FPA which is a pretty new optimization algorithm and a well-known optimization algorithm of which particle swarm optimization (PSO) to minimize the integral of time weighted absolute error (ITAE) performance index. Also, the other error-based objective functions are considered. The entire energy system and controllers are developed in Matlab/Simulink and realized experimentally. Real time applications are done through DS1104 Controller Board. The simulation and experimental results show that FPA tuned fuzzy logic controller provides lower value performance indices than conventional PID controller by reducing output voltage sags and swells of the wave/SC energy system.**

***Index Terms*—fuzzy control, heuristic algorithms, renewable energy sources, supercapacitors, DC-DC power converters.**

I. INTRODUCTION

With the increasing energy demand of the globe, countries have focused on renewable energy sources (RESs) in order to satisfy the energy demand. Considering the undesirable environmental effects and price fluctuations of fossil fuels, it is highly strengthening the idea of that the future belongs to the utilization of RESs such as wind, solar, wave, tidal and biomass etc. [1]

As an unexploited source of renewable energy, waves have the highest energy density (J/m^2) all over the globe compared to popular RESs such as solar and wind [2]. Moreover, wave energy among the other sources has low environmental impact and little energy loss while travelling the large distances. Whereas it has some design challenges while extracting the power from the sea waves because of the stochastic nature of wave dynamics and extreme weather conditions [3]. A wave energy converter (WEC) transforms motion of the sea waves into electrical energy through a generator connected to a directly coupled translator or mechanical parts. Many prototypes of the WEC systems with different power limits, efficiency, operation costs, etc. have been presented in literature. Oscillating Water Column (OWC), Pelamis, Wave Dragon and Archimedes Wave Swing (AWS) are mainly used wave energy converters [4].

Also, different types of power electronic schemes are tested for WEC systems to obtain a reliable and stable load power; AC/DC/AC converter [5], AC/DC H-bridge rectifiers [6], DC/DC converters [7, 8] and two different topologies based on AC/DC passive diode rectifier with supercapacitor filters (SCF) [9] and controlled power filters [10], etc. Because of the stochastic nature of the wave height and period, direct-drive WECs output power needs to be regulated via a storage unit and a power electronic interface circuit before the load or grid connections [11].

A SC, also known as ultra-capacitor, is a new generation storage unit that has a very high capacitance value which provides a high energy density compared to a conventional capacitor [12]. Also, compared to batteries, it has a very long cycle life, fast charging-discharging capacity, and high efficiency [13]. Operating WEC and SC in parallel, the hybrid energy system can achieve the load power demand. Without the SC unit, standalone WEC system cannot satisfy the load power requirements due to irregular wave effects that cause voltage drops and fluctuations. Integration of the SCs to a WEC system with and without power electronic devices can be found in literature [9],[14-16]. Because of the high power density of the SCs, they can directly be connected in parallel with an energy source especially for low-voltage applications (<50V) [17]. Also, direct integration of the SCs to the dc bus increases the overall system efficiency by eliminating DC/DC converter losses. Whereas the over and under charge considerations of the SC must be considered in directly connections. PID controller has been used for many years because of its feasibility and easy implementation. Whereas its performance on nonlinear systems with uncertainty and varying parameters is criticized negatively. Also, the badly tuned controller parameters decreases the controller performance. Various type of parameter adjustment methods have been introduced in literature. Some of these are based on analytical rules, adaptive methods and meta-heuristic algorithms etc. [18-21]. Fuzzy logic technology indicated an impressive achievement in solving control problems because of its advantage of using human expert knowledge [22].

This work was supported by the Research Fund of Karadeniz Technical University under Grant Number FBA-2014-5168.

Digital Object Identifier 10.4316/AECE.2017.01006

1582-7445 © 2017 AECE

[Downloaded from www.aece.ro on Saturday, October 13, 2018 at 09:10:47 (UTC) by 159.226.100.198. Redistribution subject to AECE license or copyright.]

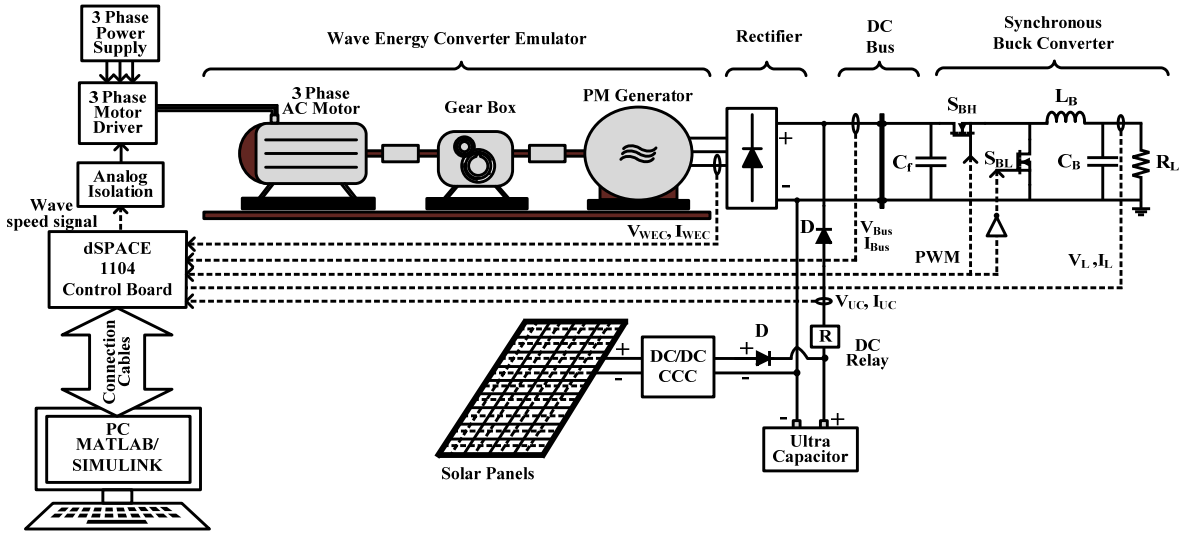


Figure 1. Schematic of the designed WEC system

However, there is not a systematic way or tune method to determine the parameters of a FLC of which complicates the design process. To overcome this problem, the advantage of optimization methods and algorithms which have several application areas such as renewable energy [23], automatic control system [24], pattern recognition [25], scheduling problems [26] can be considered.

The meta-heuristic optimization algorithms inspired by nature have been used by the researches in the parameter tuning of the FLC. Some of these algorithms are Cuckoo Search Algorithm (CSA) [27], Particle Swarm Optimization (PSO) [28], Genetic Algorithm (GA) [29], Ant Colony Optimization (ACO) [30] and Bees Algorithm (BA) [31], etc.

Recently, a new population based optimization algorithm named flower pollination algorithm (FPA) is introduced in [32]. The algorithm mimics the pollination process of the flowering plants and it provides a faster convergence rate with a powerful solution. Also, the proposed algorithm has only one key parameter (*p*: switch probability) which makes it to implement easily [32]. FPA is used in literature to optimize capacitor placement in radial systems [33], photovoltaic (PV) parameter estimation [34], optimization of PV/Wind/Battery stand-alone system [35], etc. In controller parameter tuning process, it is also used for PI-PD cascaded controller in automatic generation control [36] and PI controller for load frequency control [37].

In this study, a solar charged SC energy storage unit with a synchronous buck converter (SBC) is presented for a WEC system in irregular sea state to obtain a reliable and quality increased load power. The SBC is controlled as a power electronic interfacing circuit between the energy systems and load. A simulation model for the whole system is developed in MATLAB/Simulink/SimPower environment. The simulations are validated experimentally by using a DS 1104 Controller Board. The modelling errors are graphically illustrated for SC and SBC. Also, a recently popular optimization algorithm called flower pollination algorithm is introduced to tune the optimum parameters of a designed FLC for SBC. Integral of time weighted absolute error (ITAE) performance index is used as an objective function. In order to show the effectiveness of the FPA, a well-known optimization algorithm PSO is used for comparison in terms of corresponding iteration number and convergence rate to the optimal solution. To show a detailed comparison, the other error based performance indexes, integral of absolute error (IAE) and integral of squared error (ISE), are also considered. Proportional-integral-derivative (PID) controller is tuned by both of the search algorithms and their results are compared to those of FLC.

The rest of this paper is organized as follows. Section 2 presents the WEC system with the subtitles wave energy converter, synchronous buck converter and supercapacitor unit, respectively. The designed FLC is given in Section 3. The proposed meta-heuristic algorithms with optimization results are discussed in Section 4. Experimental results are presented in Section 5. Finally, conclusion is stated in Section 6.

II. Wave Energy Conversion System

The scheme of the proposed system shown in Fig. 1 consists of wave energy converter (WEC), passive rectifier, SC with backup solar panels, DC/DC constant current charger (CCC) for limiting of the charge current of the SC, synchronous buck converter and a resistive load.

The experimental setup of a WEC Emulator (WECE) is established in laboratory to emulate the irregular wave effects on electrical side of a WEC. A 3-phase AC motor, gear-box and 3-phase permanent magnet generator (PMG) is used to emulate the wave turbine characteristics. The parameters of these subsystems are given in Appendix.

Due to irregularities encountered in wave period and height, the generated power is also shows the same characteristic including voltage variations and drops. In order to utilize the induced power in the WEC and provide a stable voltage to the load, output voltage of the WEC is rectified and SC unit is directly connected to the WEC output. The SC unit holds the rectified WEC voltage on its charge voltage when the energy produced from waves is inadequate. Then, a SBC is controlled to regulate the load voltage. The parts of the WES are described below, respectively.

A. Wave Energy Converter

In this study, mathematical model of a permanent magnet

[Downloaded from www.aece.ro on Saturday, October 13, 2018 at 09:10:47 (UTC) by 159.226.100.198. Redistribution subject to AECE license or copyright.]

linear generator (PMLG) referred in [38] is used to simulate the WEC dynamics. The active area between the stator and translator is not considered for this study.

The flux generated by permanent magnets can be considered to have a sinusoidal form and the change of the magnetic flux with respect to time is depended on the change of the translator displacement in respond to time. Based on Faraday's law, the mathematical description of the induced three-phase voltage with $\theta_{[a,b,c]}$=[0 +2π/3 -2π/3] phase shifts is given below [38].

$$V_{[a,b,c]} = -\frac{2\pi}{\lambda} N\phi_0 \cos(\frac{2\pi}{\lambda} x + \theta_{[a,b,c]}) \frac{dx}{dt} \quad (1)$$

where λ is the wave length, ϕ_0 is the magnitude of the flux, x is the translator displacement, N is the number of turns of the windings, respectively. The above equation is used for simulating the induced 3-phase irregular wave energy which is experimentally produced in PMG.

B. Modelling of Synchronous Buck Converter

A SBC is a type of switch mode power supply (SMPS) which steps down input DC voltage to a lower value DC voltage while increasing the output current. This topology is widely used for low power applications due to its high efficiency resulting by a second switch component [39].

In this study, a SBC is designed and controlled to transferring a reliable feeding voltage to the load with increased quality. The SBC is similar to conventional buck converter. But, a second switching element is used instead of a diode in this topology. The second switch, especially a MOSFET, behaves like a small resistor in conducting mode and it increases the efficiency of the converter while reducing the power loss and voltage drop on switching element [39]. The converter topology pointed out in Fig. 2 consists of an inductor (L), switches (S_H, S_L), input (C_f) and output capacitor (C_{out}) filters. S_H is the high side and S_L is the low side mosfets which work synchronously. r_L and r_C are the equivalent parasitic resistance of inductor and capacitor, respectively. R_S and C_S are the passive R-C snubber circuit components which are used to suppress the voltage spikes during the switching moments. The converter parameters are calculated by using the equations given in [39] for a 20 kHz switching frequency.

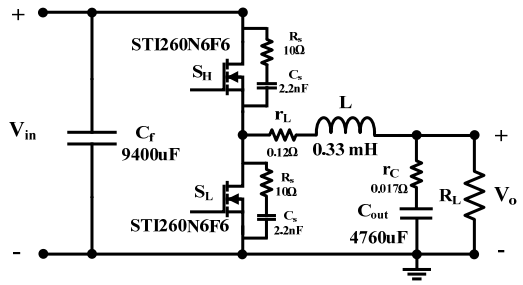


Figure 2. The equivalent circuit diagram of the designed SBC

To verify the accuracy of the modeled converter, simulation model are compared to real time experiment. A sinusoidal duty cycle (f=0.5Hz, Amplitude=0.3, Bias=0.5) is applied to the model and real-time circuit while the input voltage and load resistance are set to 12 V and 20 Ω, respectively. Fig. 3 shows the response of the simulation model and realized circuit with modeling errors. A satisfied modeling error is obtained with the simulation model of the converter.

C. Supercapacitor Energy Storage Unit

There are several types of SC mathematical models used in simulation studies. Some of well-known models are classical R-C model [40, 41], R-C parallel branch model [41], R-C transmission line model [42], and R-C series-parallel branch model [43], etc. All the aforementioned models have advantages and disadvantages with respect to each other [44].

In this study, the classical R-C model of which equivalent circuit shown in Fig. 4 is used to simulate the dynamics of a SC. The reasons to prefer this topology are that it is easy to model and suitable for slow discharging applications and pulse loads [45].

The model consists of an equivalent series resistance (R_{esr}) which is the internal resistance of the capacitor, an equivalent parallel resistance (R_{epr}) representing the leakage currents and C is the capacitance. The following equation gives the relationship between the SC voltage and current.

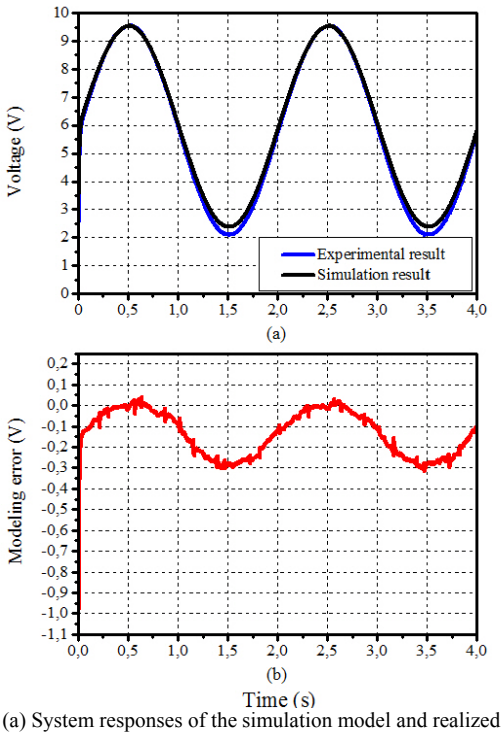


Figure 3. (a) System responses of the simulation model and realized circuit, (b) modeling error

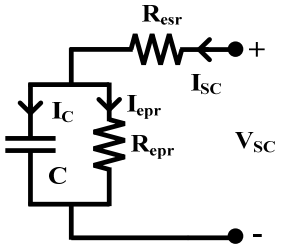


Figure 4. Equivalent electrical circuit of a R-C modeled SC

$$V_{SC}(t) = I_{SC}(t)R_{esr} + \frac{1}{C}\int_0^t I_C(t)dt + V_{SC(i)}(t) \quad (2)$$

Where V_{SC} is the terminal voltage, I_{SC} is the current flowing through the SC, and $V_{SC(i)}$ is the initial voltage of the capacitance, respectively. In order to obtain high voltage-current ratings, series-parallel configurations of the SC cells are used to form the SC module. In this study, Maxwell

[Downloaded from www.aece.ro on Saturday, October 13, 2018 at 09:10:47 (UTC) by 159.226.100.198. Redistribution subject to AECE license or copyright.]

BMOD0083-P048 SC module is used [46].

The comparison of the simulation and the experimental data for discharging of the SC is shown in Fig. 5 with different discharging resistive loads. When the voltage of the SC is nearly decreased to 12 V, the load (50 Ω) is reduced to half of it (25 Ω). The experimental and simulation results seem to be consistent.

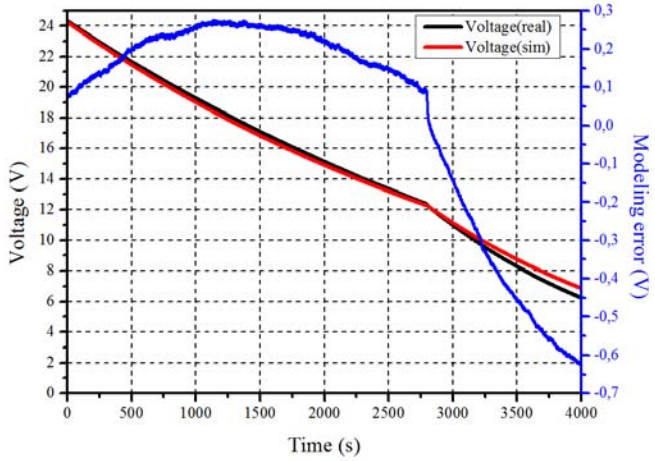


Figure 5. SC discharging voltage with modeling error

III. Fuzzy Logic Controller

The fuzzy logic technology proposed by Zadeh [22] is highly preferred in many control problems because of its ability to solve nonlinear and complex control problems without requiring the knowledge of the system to be controlled. The FLC provides a human reasoning and decision making in the format of fuzzy rules. The FLC consists of three main processes which are *fuzzification*, *rule base-reasoning* and *defuzzification* sections.

In *fuzzification* process, crisp input values of error (e) and its change (de) are fuzzified by triangle membership functions (MF) [47].

The subsets of the MF are named as negative big (NB), negative small (NS), zero (Z), positive small (PS) and positive big (PB), respectively. The scaling factors of these subsets directly affect the performance of the FLC. MFs are scaled by the constants G_e and G_{de} for the inputs and G_{du} for the output. Illustrated fuzzy sets are depicted in Fig. 6.

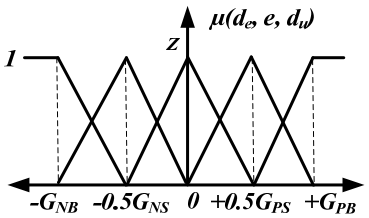


Figure 6. MFs for inputs and output of the FLC

A *knowledge base* consists of rules related with system. The rules are based on *if-then-else* structure. A symmetrical rule table shown in Table I including twenty-five rules is used for this study.

TABLE I. Rule Table of the Designed FLC

		Change of error (d_e)				
		NB	**NS**	**Z**	**PS**	**PB**
Error (e)	**NB**	NB	NB	NS	NS	Z
	NS	NB	NS	NS	Z	PS
	Z	NS	NS	Z	PS	PS
	PS	NS	Z	PS	PS	PB
	PB	Z	PS	PS	PB	PB

These fuzzy rules are employed by Mamdani's max-min method as the inference system [48].

After *fuzzification* and *rule base* stages, crisp control signal is calculated by using the center of area (COA) method which is widely used in FLC applications [49].

All FLC algorithms based on the mathematical equations are designed by using MATLAB/Simulink blocks instead of a FLC Toolbox and the detailed design information about the FLC used in this study is given in [50]. A generalized view of the designed FLC is depicted in Fig. 7.

IV. Optimization Algorithms

In this study, the optimization problem is to minimize objective function (ITAE) in order to get maximum performance in terms of transient and steady-state responses of the system. Therefore, the parameters of the controllers are required to be tuned optimally.

We designed an optimized FLC by employing the FPA. The parameters of the FLC (G_e, G_{de}, and G_{du}) are used to scale the membership functions of the FLC for inputs and output. Since these parameters are directly affect the performance of the FLC, their optimum values are searched by FPA. An error-based performance index which is integral of time-weighted absolute error (ITAE) is used as an objective function. The control parameters which make the ITAE value minimum are selected as the optimal controller parameters. The reason for selecting ITAE criteria as a cost function is that it produces smaller overshoot and oscillations than the other error-based performance indexes [51]. Also, the other error based performance indices integral of absolute error (IAE) and integral of squared error (ISE) are considered for a detailed comparison. The mathematical equations of these objective functions are given in (3), (4) and (5), respectively.

$$ITAE = \int_0^t t\left|e(t)\right| dt \tag{3}$$

$$IAE = \int_0^t \left|e(t)\right| dt \tag{4}$$

$$ISE = \int_0^t e(t)^2 dt \tag{5}$$

where e(t) is the error which is the difference between the reference signal and measured output signal.

The performance of the FPA is compared to PSO which is performed under the same optimization process. Also, two different optimized PID controllers by FPA and PSO algorithm are designed to compare the performance of the designed FLCs.

A. Flower Pollination Algorithm

Flower pollination algorithm (FPA) proposed by Yang [32] is a new metaheuristic problem solution algorithm based on pollination process of the flowering plants. There are two type pollination methods in nature: *cross* and *self-pollination*. The cross-pollination is observed between different types of plants. This means pollen of a flowering plant fertilizes a different plant. Whereas, in the self-pollination, fertilization is occurred in genetically similar flowers [32].

[Downloaded from www.aece.ro on Saturday, October 13, 2018 at 09:10:47 (UTC) by 159.226.100.198. Redistribution subject to AECE license or copyright.]

Also, transferring of pollens seems in two major ways. These are abiotic and biotic forms. If the pollens are transferred by pollinators which are the pollen carriers such as insects and animals, it is called as biotic and 90% of the pollination of flowering plants occurs in biotic form [32]. Without any pollinators, the pollination process is called as abiotic. By using the above explained definitions, the algorithm is summarized in four basic rules [32]. The first rule is that biotic and cross-pollination are considered as global pollination process. In this process, pollinators obey a levy distribution.

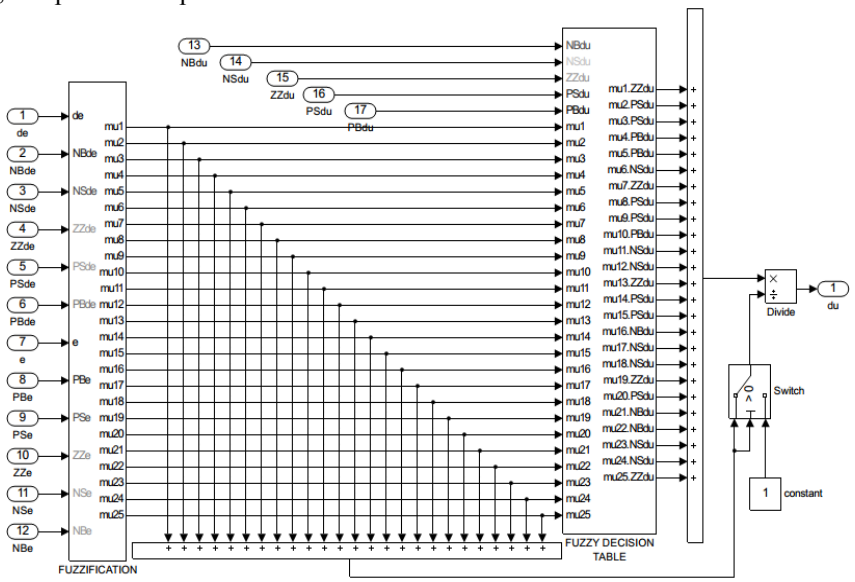


Figure 7. A generalized view of the designed FLC

Abiotic and self-pollination are used for local pollination for the second rule. The third rule is that pollinators especially honeybees (flower constancy) can be considered as the reproduction probability which is proportional to the similarity of two flowers involved. The final rule is the switch probability ($0 \leq p \leq 1$) which is a threshold value that controls the switching or interaction between the local and global pollination. The rules given above are required to be described in mathematical forms.

Firstly, the equation of the global pollination (Rule 1) and flower constancy can be written as [32]:

$$x_i^{t+1} = x_i^t + \gamma L(\lambda)(x_i^t - g_{best}) \tag{6}$$

where t is the iteration number, g_{best} is the current smallest fitness function value, γ is the scaling factor considered as step size, x_i^t is the pollen and $L(\lambda)$ is the Levy flight based step size. Levy flight of which equation given below is used to simulate the long distances that is covered by insects with different step sizes [32] ($S>>S_0>0$).

$$L \sim \frac{\lambda \Gamma(\lambda) \sin(\pi\lambda/2)}{\pi} \frac{1}{S^{1+\lambda}} \tag{7}$$

$\Gamma(\lambda)$ is the gamma function and it is valid for large steps (S>0). The Rule (2) and (3) for local pollination are explained by:

$$x_i^{t+1} = x_i^t + \in (x_j^t - x_k^t) \tag{8}$$

where x_j^t and x_k^t are pollens from different flowers which are genetically similar. This simulates the flower constancy in a limited neighborhood considered as the local pollination and it is drawn by ϵ from a uniform distribution [0, 1] [32]. Since, flower pollination can occur at all scales, both local and global, a switch probability describes Rule (4) which is used to emulate to switch between global pollination to intense local pollination [32]. The flowchart of the FPA algorithm is depicted in Fig. 8 (a).

B. Particle Swarm Optimization Algorithm

The PSO algorithm developed by Kennedy and Eberhart [52] is one of the well-known metaheuristic algorithms and it is mostly used to solve nonlinear complex optimization problems. The algorithm simulates the movements of the fish schooling or bird flocking by using position (X) and velocity (V) equations given in (9) and (10), respectively.

Each particle in population keeps its coordinates which corresponds the best solution searched so far. This value is called as p_{best}. The comparison of the all p_{best} of the particles results the g_{best} which is obtained overall best value so far in the population [52]. p_{best} and g_{best} values are updated at each iteration until the algorithm ends.

$$V_{id}(k+1) = w(k)V_{id}(k) + c_1 r_1(pbest(k) - X_{id}(k)) + c_2 r_2(gbest(k) - X_{id}(k)) \tag{9}$$

$$X_{id}(k+1) = X_{id}(k) + V_{id}(k+1) \tag{10}$$

where V_{id} and X_{id} are the velocity and position of the i^{th} particle in the d dimensional space, k is the iteration number, c_1 and c_2 are acceleration factors, r_1 and r_2 are the random numbers in the range of [0, 1], w is the inertia weight The flowchart of the PSO algorithm is given in Fig 8(b).

C. Optimization Process and Results

The parameters of the FLC and PID controller are tuned by both FPA and PSO algorithm in Matlab/Simulink environment. In optimization process, load variations are not considered in simulation and the load is set to 20 Ω. Load variations are considered for experimental validation in order to show the effectiveness of the designed controllers with optimized parameters. The controller parameters are optimized for the system with a 12 V initial charged SC unit.

[Downloaded from www.aece.ro on Saturday, October 13, 2018 at 09:10:47 (UTC) by 159.226.100.198. Redistribution subject to AECE license or copyright.]

For a fear comparison, population size (n) and iteration number (N) are set to 10 and 50 for both of the algorithms, respectively. The search spaces for the controller parameters and the value of the algorithm parameters for PSO and FPA are also given in Appendix.

Firstly, the FLC parameters (G_{de}, G_e, G_{du}) are tuned by using FPA and PSO. Both of the algorithms are performed for 5 times. Performances of the optimization algorithms are compared each other in terms of minimum cost function $f(\theta)$ and its corresponding iteration number (*CIN*) for each simulation.

The simulation results of the trials with the averaged values of $f(\theta)$ and *CIN* are given in Table II.

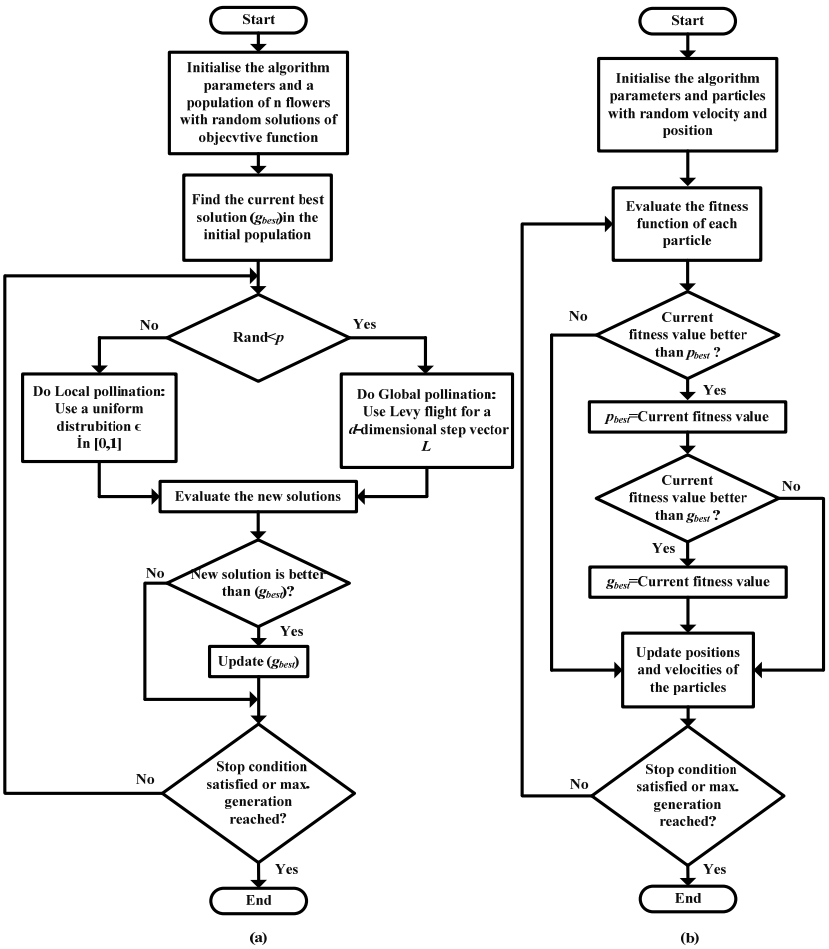


Figure 8. Flowchart of the algorithms (a) FPA, (b) PSO

TABLE II. PERFORMANCE COMPARISONS OF THE ALGORITHMS FOR FLC

FLC	Trials for FPA					Average values	
	1	2	3	4	5	f(θ)	CIN
f(θ)	11.21	10.22	6.29	6.50	11.98	9.24	20.4
CIN	16	22	21	25	18		
FLC	Trials for PSO					Average values	
	1	2	3	4	5	f(θ)	CIN
f(θ)	12.62	8.623	11.32	7.46	7.782	9.56	33.4
CIN	27	32	43	36	29		

Comparison results for the best trial of the algorithm for FLC are that FPA converges to its optimal solution 6.29 at 21th iteration for the third test, whereas PSO converges to its optimal solution 7.46 at 36th iteration for the fourth test. Considering the average values, it is observed that FPA provides a better convergence rate to the optimal solution and a lower cost function than PSO algorithm in general. The best trial of the FPA and PSO for the FLC parameter tuning is shown in Fig. 9. The optimized FLC parameters obtained in the best trial are given in Table III with the performance indexes.

TABLE III. OPTIMIZED FLC PARAMETERS

FLC	Controller Parameters			Performance indexes		
	G_{DE}	G_E	G_{DU}	ITAE	ISE	IAE
FPA	0.0761	0.216	27.37	6.29	0.0247	0.229
PSO	0.0379	0.195	29.12	7.46	0.0306	0.284

In order to compare the performance of the FLC, a conventional PID controller with the parameters K_P, K_I and K_D is also designed and tuned by FPA and PSO algorithm. The number of trials and iterations are the same as in FLC optimization process. The results of trials done for PID controller are given in Table IV. Algorithms are compared in terms of minimum value of the objective function ($f(\theta)$) and its corresponding iteration number (*CIN*) for each trial. The simulation results of the trials with averaged values of $f(\theta)$ and *CIN* are also given in Table IV.

The best obtained trial result for both of the algorithms is show that the FPA converges to its minimum objective function value 8.48 at 17th iteration for the second test, whereas PSO converges to its optimal solution 9.27 at 34th iteration for the fifth test. The change of objective function of the best trial of both algorithms is shown in Fig. 10.

[Downloaded from www.aece.ro on Saturday, October 13, 2018 at 09:10:47 (UTC) by 159.226.100.198. Redistribution subject to AECE license or copyright.]

Averaged values of objective function and corresponding iteration number for PID tuning shows the superiority of the FPA compared to the PSO results.

TABLE IV. PERFORMANCE COMPARISONS OF THE ALGORITHMS FOR PID

PID	Tests of FPA					Average values	
	1	2	3	4	5	f(θ)	CIN
f(θ)	9.82	8.48	13.32	9.69	13.38	10.93	21.2
CIN	15	17	26	23	25		
PID	Tests of PSO					Average values	
	1	2	3	4	5	f(θ)	CIN
f(θ)	24.18	11.53	16.04	20.17	9.27	16.23	29.0
CIN	29	24	31	27	34		

The optimized parameters for the PID controller obtained in the best trial are given in Table V. As the performance of the FLC and PID controller tuned by the FPA is better than the PSO one in terms of the cost function, the FPA tuned FLC and PID controller are implemented experimentally.

TABLE V. OPTIMIZED PID PARAMETERS

PID	Controller Parameters			Performance indexes		
	K_P	K_I	K_D	ITAE	ISE	IAE
FPA	32.308	8.3748	0.148	8.48	0.03617	0.3768
PSO	48.230	19.44	0.24	9.27	0.04326	0.4146

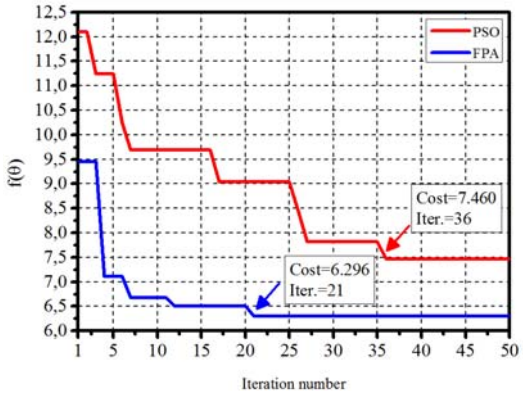


Figure 9. Change of the objective functions with PSO and FPA for the FLC for the best trials

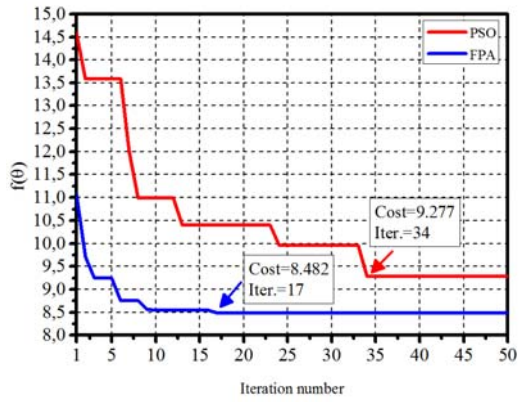


Figure 10. Change of the objective functions with PSO and FPA for the PID controller for the best trials

V. EXPERIMENTAL SET UP AND RESULTS

Modeling success of the SBC and SC storage unit were demonstrated in section II. The designed controller using these models were given in optimization process and results in detail. In this section, in order to validate our theoretical results, we present the experimental set up and obtained results.

The designed WEC system shown in Fig. 1 is modeled in Matlab/Simulink environment. The datasheet values for the electrical components are used in simulation. The simulation of the energy extracted from irregular waves are performed by using the equation (1). SC unit and DC-DC converter are modeled with an acceptable modelling success. In order to use the FLC toolbox in Matlab, we design a FLC by using common used blocks of Simulink software.

The performance of the optimized controllers by FPA and PSO algorithm are investigated for both real time and simulation in terms of objective function. Since, the lowest performance index is obtained by using FPA tuned FLC, the all experimental results are shown with FPA tuned FLC. Also, FPA tuned PID controller is compared to FLC one for load voltage.

The implementation of the control algorithms and acquisition of the voltage-current data is realized by a DS1104 Controller Board. Galvanic isolated voltage-current transducers are used to transfer the real time voltage-current data to the computer. The experimental setup is shown in Fig. 11.

To show the effect of the modelled SC, two different experiments were performed with and without the SC energy storage bank. The WEC phase to phase voltage and phase current with and without SC unit is pointed out in Fig. 12. The DC bus voltage and current is shown in Fig. 13 with and without SC.

The effect of the SC is shown in Fig. 12 on the WEC phase current. WEC provides energy to the load when the induced voltage value is greater than 11.16 V. The total DC relay and the diode voltage drops are calculated approximately 0.8V.

Fig. 13 shows that the SC unit charged to 12 V by solar panels eliminates the voltage drops seen in irregular wave effects on a WEC. Therefore, a more stable DC bus voltage is obtained for the input of the SBC. Then, the SBC converts variable DC bus voltage to a lower value of 5 V for the 20 Ω load.

Fig. 14 shows the load voltage and current with and without SC bank. The standalone WEC can not meet the load power requirements without SC because of the zero-crossing points of WEC. The comparision of the FPA tuned FLC and PID controller are given in Fig. 15 with the zoomed parts. The FLC provides a lower overshoot compared to PID controller. Also, FLC provides a stable voltage with increased quality to the load.

Experimental performance result comparisions for FPA tuned FLC and PID are given in Table VI. The performance indices are calculated with a charged 12 V SC unit connected to the DC bus.

TABLE VI. EXPERIMENTAL PERFORMANCE RESULTS OF THE CONTROLLERS

Controller type	Performance indexes		
	ITAE	ISE	IAE
FLC	10.60	1.8017	0.8415
PID	28.454	1.8213	1.5438

It is indicated in Table VI that FLC provides lower value performance indices than the PID controller in experimental tests. In Fig. 16 and Fig. 17, the designed WEC system is tested with a decreased load resistance of 6.25 Ω and different initial SC charge voltages. The discharging of the SC while the DC bus current increasing can be seen from these figures clearly.

[Downloaded from www.aece.ro on Saturday, October 13, 2018 at 09:10:47 (UTC) by 159.226.100.198. Redistribution subject to AECE license or copyright.]

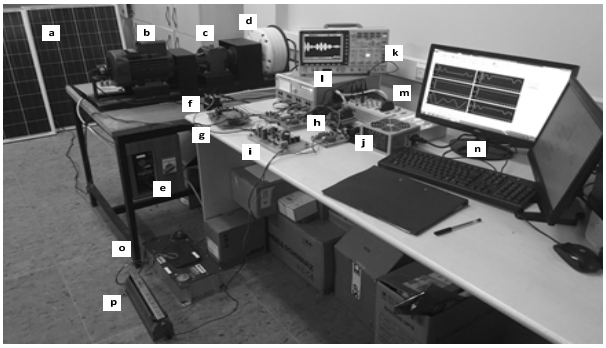


Figure 11. Experimental set up; (a) solar panels, (b) 3-phase motor, (c) gearwheel, (d) PM Generator, (e) frequency driver,(f) rectifier, (g) SC charge circuit, (h) voltage-current transducers, (i) SBC circuit, (j) symmetric power supply, (k) oscilloscope, (l) power supply, (m) DS 1104, (n) computer, (o) SC unit, (p) resistive load

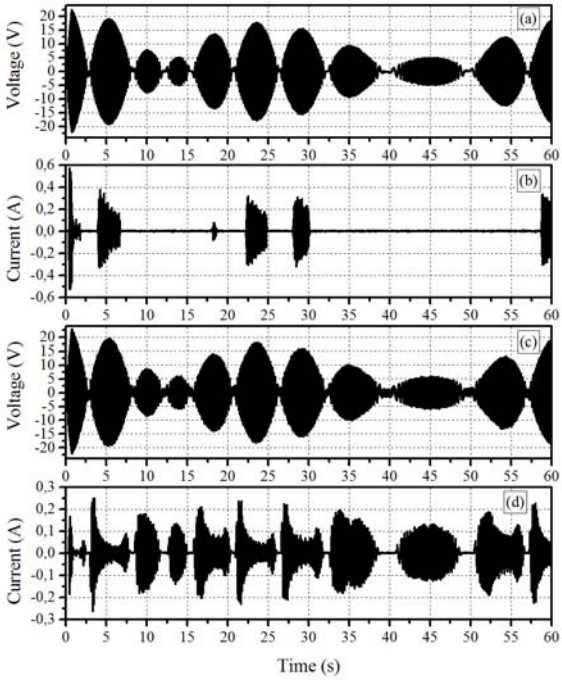


Figure 12. Experimental results of the WEC phase to phase voltage and phase current with (a, b) and without (c, d) SC unit

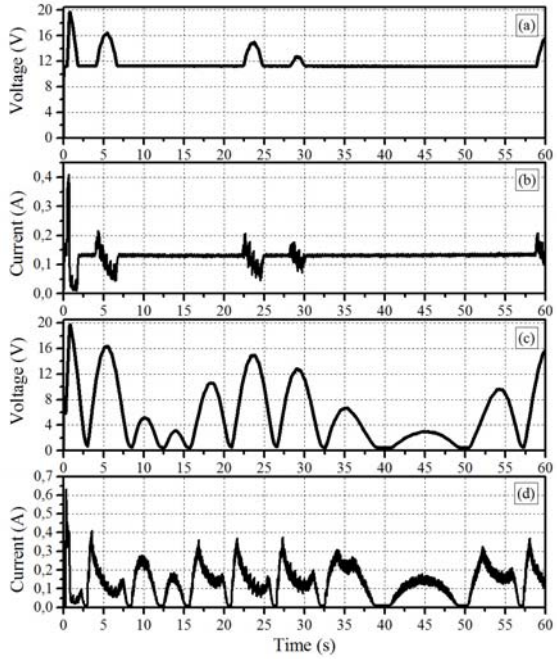


Figure 13. Experimental results of the DC-bus voltage and current with (a, b) and without (c, d) SC unit

VI. Conclusion

In this study a solar charged supercapacitor (SC) storage unit with a synchronous buck converter (SBC) is presented for a wave energy conversion system (WECS). Because of the irregularities observed in real sea waves, direct-drive WECs are inefficient to provide a stable and reliable power to the load. Therefore, they needs an extra storage unit or a power supply with power electronic devices.

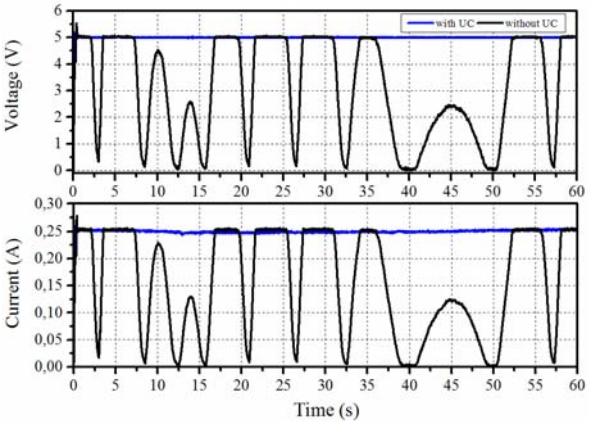


Figure 14. Experimental results of the load voltage and current with and without SC unit

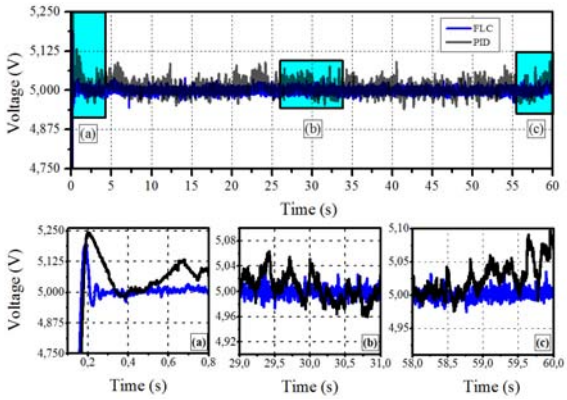


Figure 15. Experimental results of the FPA tuned FLC and PID controlled load voltage with SC unit

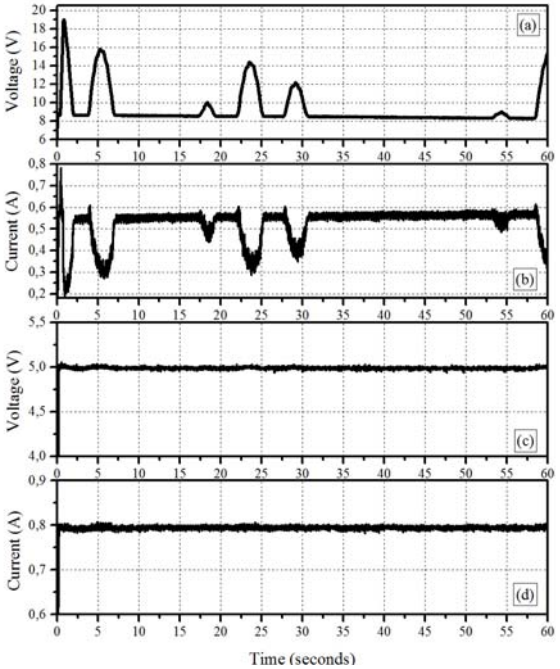


Figure 16. Experimental results of the DC bus voltage (a), DC bus current (b), load voltage (c) and load current (d) with SC (SC charge voltage is 9.78V, load is 6.25Ω)

[Downloaded from www.aece.ro on Saturday, October 13, 2018 at 09:10:47 (UTC) by 159.226.100.198. Redistribution subject to AECE license or copyright.]

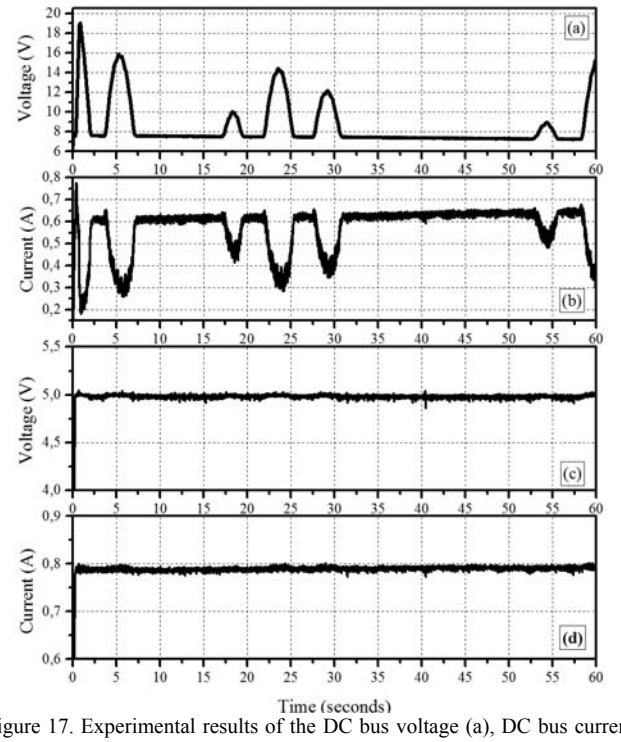


Figure 17. Experimental results of the DC bus voltage (a), DC bus current (b), load voltage (c) and load current (d) with SC (SC charge voltage is 8.8V, load is 6.25Ω)

A SC unit is modeled and used with a SBC to eliminate the voltage drops and fluctuations seen in WEC system for irregular sea wave conditions. The SBC simulation model is compared to experimental converter data. The results show that the simulation model provides consistent result. For further reduction of the modeling error of the SBC, fractional order modeling may be considered.

The rectified WEC output voltage is integrated with SC unit. Since the small-scale on-shore waves are considered in this study, WEC output power is insufficient to charge SC unit. So, solar panels are used to increase the charge capacity of the UC. Then, the variable DC-bus voltage is applied to the SBC. The SBC is controlled by a designed FLC. Also, a PID controller is used for comparison.

The WEC system is tested for different initial SC charge voltage with decreased load resistance (Fig. 16 and Fig. 17). Under this case, SBC succeed to transfer stable energy to the load.

In optimization process, a newer algorithm FPA and a well-known algorithm PSO are utilized in order to obtain the best controller performances. The ITAE is considered as a cost function and the other error-based performance indices are used for a detailed comparison for the controllers. The simulation results show that the FPA provides a lower performance index with a faster convergence rate than the PSO algorithm for both of FLC and PID controller. The performance results show the superiority of the FLC over the classical PID controller. The simulation study is validated experimentally and consistent results are observed.

The SC has lots of superiorities compared to a conventional battery. Whereas, its energy density is lower than a battery and the cost of it is slightly higher. The use of the SC in energy systems will increase much more than today when the cost and energy density problems are solved. In this study, a SC is modeled by using classical RC model. The modeling error shown in Fig. 5 can be reduced by using the different modeling types as recommended in SC modeling section. A constant current charger (CCC) is used to limit the charging current of SC. Also, a solid-state relay is connected in series to the SC in order to save the circuits and SC in case of short circuit. Since the PV system is just employed to charge the UC bank, it is not discussed in this study.

APPENDIX

SC parameters:
Rated capacitance C=83 F, R_{ESR}=10 mΩ,
Rated voltage V=48 V, Power density=2700 W/kg,
Max. energy density=2.6 Wh/kg, Mass=10.3 kg
Gear specifications:
Conversion rate=4
3-phase motor specifications:
Nominal power=1.5 kW, Nominal speed=1440 rpm,
Nominal current=3.3 A, Nominal moment=4 Nm
3-phase permanent magnet generator specifications:
Nominal power=1.5 kW, Nominal speed=550 rpm,
Phase resistance=5 Ω, Phase inductance=18.2 mH,
Pole number=8, Torque constant=1.1 Nm/A,
Speed constant=11.5 rpm/V, Rotor inertia=0.011 kgm^2,
Magnet type: NdFeB (Neodyum Iron Boron),
Generator arrangement: 3-phase star connected-AA output
FPA parameters:
p=0.65, γ =0.15, λ=1.25
PSO parameters:
c_1 and c_2=2, w=0.7
Interval for the optimized parameter of PID and FLC
$0.001<K_P<50$, $0.0001<G_{DE}<1$
$0.001<K_I<25$, $0.0001<G_E<5$
$0.001<K_D<1$, $0.0001<G_{DU}<30$

REFERENCES

[1] S. R. Bull, "Renewable energy today and tomorrow," in Proc. of the IEEE, vol. 89, no. 8, pp. 1216-1226, 2001. doi:10.1109/5.940290

[2] A. Muetze, J. G. Vining, "Ocean wave energy conversion-a survey," 41st Industry Applications Conference (IAS), vol. 3, pp.1410-1417, Oct. 2006. doi:10.1109/IAS.2006.256715

[3] B. Czech, P. Bauer, "Wave energy converter concepts: design challenges and classification," IEEE Trans. Ind. Elect., vol. 6, no. 2, pp. 4-16, Jun 2012. doi:10.1109/MIE.2012.2193290

[4] E. Ozkop, I. H. Altas, "Control, power and electrical components in wave energy conversion systems: A review of the technologies," Renewable and Sustainable Energy Reviews, vol. 67, pp. 106-115, 2017. doi:http://dx.doi.org/10.1016/j.rser.2016.09.012

[5] M. Jasinski, M. Malinowski, M. P. Kazmierkowski, H. C. Soerensen, E. FriisMadsen, D. Swierczynski, "Control of AC/DC/AC converter for multi MW wave dragon offshore energy conversion system," IEEE Int. Symp. Industrial Electronics (ISIE), pp. 2685–2690, 2007. doi:10.1109/ISIE.2007.4375032

[6] Z. Nie, P. C. J. Clifton, R. A. Mc Mohan, "Wave Energy Emulator and AC/DC Rectifiers for Direct Drive Wave Energy Converters," 4th IET Conference on Power Electronics, Machines and Drives, pp. 71-75, 2-4 April 2008. doi:10.1049/cp:20080485

[7] S. Hazra, S. Bhatacharya, "Short time power smoothing of a low power wave energy system," 38th IEEE Industrial Electronic Society Conference, pp. 5846-5851, 25-28 Oct. 2012. doi:10.1109/IECON.2012.6389128

[8] F. Wu et all, "Modeling, control strategy and power conditioning for direct-drive wave energy conversion to operate with power grid," in Proc. of the IEEE, vol. 101, no. 4, pp. 925- 941, 2013. doi:10.1109/JPROC.2012.2235811

[9] C. Boström, E. Lejerskog, M. Stalberg, K. Thorburn, M. Leijon, "Experimental results of rectification and filtration from an offshore wave energy system," Renewable Energy, vol. 34, no. 5, pp. 1381-1387, 2009. doi:http://dx.doi.org/10.1016/j.renene.2008.09.010

[10] E. Ozkop, I. H. Altas, A. M. Sharaf, "A novel switched power filter-green plug (spf-gp) scheme for wave energy systems," Renewable Energy, vol. 44, pp. 340-358, Aug. 2012. doi:http://dx.doi.org/10.1016/j.renene.2012.01.103

[11] Y. Hong et al., "Review on electrical control strategies for wave energy converting systems." Renewable and Sustainable Energy

[Downloaded from www.aece.ro on Saturday, October 13, 2018 at 09:10:47 (UTC) by 159.226.100.198. Redistribution subject to AECE license or copyright.]

Reviews, vol. 31, pp. 329-342, Mar. 2014. doi:http://dx.doi.org/10.1016/j.rser.2013.11.053

[12] A. Burke, "Ultra capacitors: why, how and where is the technology," Journal of Power Sources, vol. 91, no. 1, pp. 37–50, Nov. 2000. doi:http://dx.doi.org/10.1016/S0378-7753(00)00485-7

[13] B.E. Conway, "Electrochemical supercapacitors: scientific fundamentals and technological applications," Kluwer Academic Publishers/Plenum Publisher, pp. 11 -31, New York, 2013.

[14] S. Hazra, S. Bhattacharya, "Short time power smoothing of a low power wave energy system," 38th Annual Conference on IEEE Industrial Electronics Society (IECON), pp. 5846-5851, 2012. doi:10.1109/IECON.2012.6389128

[15] D. B. Murray, J. G. Hayes, D. L. O'Sullivan, M. G. Egan, "Supercapacitor testing for power smoothing in a variable speed offshore wave energy converter," Oceanic Engineering, vol. 37, no. 2, pp. 301-308, 2012. doi:10.1109/JOE.2012.2188157

[16] T. Kovaltchouk, B. Multon, H. B. Ahmed, J. Aubry, P. Venet, "Enhanced aging model for supercapacitors taking into account power cycling: application to the sizing of an energy storage system in a direct wave energy converter." IEEE Trans. on Industry Applications, vol. 51, no. 3, pp. 2405-2414, 2015. doi:10.1109/TIA.2014.2369817

[17] M. Uzunoglu, M. S. Alam, "Dynamic modeling, design, and simulation of a combined PEM fuel cell and ultracapacitor system for stand-alone residential applications," IEEE Trans. on Energy Conversion, vol. 21, no. 3, pp. 767-775, 2006. doi:10.1109/TEC.2006.875468

[18] Q.B. Jin, Q. Liu, "IMC-PID design based on model matching approach and closed-loop shaping," ISA transactions, vol. 53, no. 2, pp.462-473, 2014. doi: 10.1016/j.isatra.2013.11.005

[19] A. Besançon Voda, "Iterative auto-calibration of digital controllers: Methodology and applications," Control Engineering Practice, vol. 6, no. 3, pp.345-358, 1998. doi: 10.1016/S0967-0661(98)00005-7

[20] R. C. Panda, C. C. Yu, H. P. Huang, "PID tuning rules for SOPDT systems: Review and some new results," ISA transactions, vol. 43, no. 2, pp.283-295, 2004. doi: 10.1016/S0019-0578(07)60037-8

[21] R. E. Precup, S. Preitl, M. Balas, V. Balas, "Fuzzy controllers for tire slip control in anti-lock braking systems," IEEE Int. Con. on. Fuzzy Systems, vol. 3, pp. 1317-1322, 2004. doi: 10.1109/FUZZY.2004.1375359

[22] L. A. Zadeh, "Fuzzy sets," Information and Control, vol. 8, no. 3, pp. 338–353, 1965. doi:10.1016/S0019-9958(65)90241-X

[23] E. A. Bossanyi, "Wind turbine control for load reduction," Wind Energy, vol. 6, no. 3, pp. 229-244, 2003. doi: 10.1002/we.95

[24] R. E. Precup, S. Preitl, "Optimization criteria in development of fuzzy controllers with dynamics," Engineering Applications of Artificial Intelligence, vol. 17, no. 6, pp. 661-674, 2004. doi: http://dx.doi.org/10.1016/j.engappai.2004.08.004

[25] M. A. Ramirez-Ortegon, V. Margner, E. Cuevas, R. Rojas, "An optimization for binarization methods by removing binary artifacts," Pattern Recognition Letters, vol. 34, no. 11, pp. 1299-1306, 2013. doi: http://dx.doi.org/10.1016/j.patrec.2013.04.007

[26] S. B. Ghosn, F. Drouby, H. M. Harmanani, "A Parallel Genetic Algorithm for the Open-Shop Scheduling Problem Using Deterministic and Random Moves," International Journal of Artificial Intelligence, vol. 14, no. 1, pp. 130-144, 2016. doi:10.1145/1639809.1639841

[27] M. S. Ayas, I. H. Altas, "Fuzzy logic based adaptive admittance control of a redundantly actuated ankle rehabilitation robot," Control Engineering Practice, vol. 59, pp. 44-54, 2017. doi: http://dx.doi.org/10.1016/j.conengprac.2016.11.015

[28] S. Safari, M. M. Ardehali, M. J. Sirizi, "Particle swarm optimization based fuzzy logic controller for autonomous green power energy system with hydrogen storage," Energy Conversion and Management vol. 65, pp. 41-49, 2013. doi:http://dx.doi.org/10.1016/j.enconman.2012.08.012

[29] M. N. Uddin, M. A. Abido, M. A. Rahman, "Real-time performance evaluation of a genetic-algorithm-based fuzzy logic controller for IPM motor drives," IEEE Trans. on Industry Applications, vol. 41, no. 1, pp. 246–252, 2005. doi:10.1109/TIA.2004.840995

[30] O. Castillo, H. Neyoy, J. Soria, M. Garcia, F. Valdez, "Dynamic fuzzy logic parameter tuning for ACO and its application in the fuzzy logic control of an autonomous mobile robot," International Journal of Advanced Robotics Systems, vol. 19, pp. 1–10, 2013. doi:10.5772/54833

[31] D. T. Pham, A. Haj Darwish, E. E. Eldukhri, "Optimization of a fuzzy logic controller using the bees algorithm," International Journal of Computer Aided Engineering and Technology, vol. 1, no. 2, pp. 250-264, 2009. doi:http://dx.doi.org/10.1504/IJCAET.2009.02279

[32] X. S. Yang, "Flower pollination algorithm for global optimization," International Conference on Unconventional Computation and Natural Computation, pp. 240-249, 2012. doi:10.1007/978-3-642-32894-7_27

[33] A. Y. Abdelaziz, E. S. Ali, S. A. Elazim. "Flower pollination algorithm and loss sensitivity factors for optimal sizing and placement of capacitors in radial distribution systems." International Journal of Electrical Power & Energy Systems, vol. 78, pp. 207-214, 2016. doi:http://dx.doi.org/10.1016/j.ijepes.2015.11.059

[34] D. F. Alam, D. A. Yousri, M. B. Eteiba, "Flower pollination algorithm based solar PV parameter estimation," Energy Conversion and Management, vol. 101, pp. 410-422, 2015. doi:http://dx.doi.org/10.1016/j.enconman.2015.05.074

[35] M. Tahani, N. Babayan, A. Pouyaei, "Optimization of PV/Wind/Battery stand-alone system, using hybrid FPA/SA algorithm and CFD simulation, case study: Tehran," Energy Conversion and Management, vol. 106, pp. 644-659, 2015. doi:http://dx.doi.org/10.1016/j.enconman.2015.10.011

[36] P. Dash, L. C. Saikia, N. Sinha, "Flower pollination algorithm optimized PI-PD cascade controller in automatic generation control of a multi-area power system," International Journal of Electrical Power & Energy Systems, vol. 82, pp. 19-28, 2016. doi:http://dx.doi.org/10.1016/j.ijepes.2016.02.028

[37] D. Lakshmi, A. P. Fathima, R. Muthu, "A novel flower pollination algorithm to solve load frequency control for a hydro-thermal deregulated power system," Circuits and Systems, vol. 7, no. 4, pp. 166-178, 2016. doi:10.4236/cs.2016.74016

[38] Y. Hong, M. Eriksson, V. Castellucci, C. Boström, R. Waters, "Linear generator-based wave energy converter model with experimental verification and three loading strategies," IET Renewable Power Generation, vol. 10, no. 3, pp. 349-359, 2016. doi:10.1049/iet-rpg.2015.0117

[39] M. K. Kazimierczuk, "Pulse-width modulated DC-DC power converters," John Wiley & Sons, pp. 22-85, 2015.

[40] R. L. Spyker, R. M. Nelm, "Classical equivalent circuit parameters for a double-layer capacitor," IEEE Trans. on Aerospace and Electronic Systems, vol. 36, no. 3, pp. 829-836, 2000. doi:10.1109/7.869502

[41] L. Zubieta, R. Boner, "Characterization of double-layer capacitors for power electronics applications," IEEE Trans. on Industry Applications, vol. 36, no. 1, pp.199-205, Jan. 2000. doi:10.1109/28.821816

[42] R. De Levie, "On porous electrodes in electrolyte solutions: I. Capacitance effects," Electrochimica Acta, vol. 8, no. 10, pp. 751-780, 1963. doi:10.1016/0013-4686(63)80042-0

[43] S. Buller, E. Karden, D. Kok, and R. W. De Doncker, "Modeling the dynamic behavior of supercapacitors using impedance spectroscopy," IEEE Trans. on Industry Applications, vol. 38, no. 6, pp.1622-1626, Nov./Dec.2002. doi:10.1109/IAS.2001.955972

[44] L. Shi, M. L. Crow, "Comparison of ultracapacitor electric circuit models," IEEE Conversion and Delivery of Electrical Energy General Meeting, pp. 1-6, 2008. doi:10.1109/PES.2008.4596576

[45] R. M. Nelms, D. R. Cahela, B. J. Tatarchuk, "Modeling double-layer capacitor behavior using ladder circuits," IEEE Trans. on Aerospace and Electronic Systems, vol. 39, no. 2, pp. 430-438, 2003. doi:10.1109/TAES.2003.1207255

[46] Maxwell Technologies, BMOD0083-P048 ultracapacitor datasheet, [Online]. Available: www.maxwell.com, accessed Feb. 8, 2016.

[47] G. Klir, B. Yuan, "Fuzzy sets and fuzzy logic," New Jersey: Prentice Hall, pp. 20-51, 1995.

[48] C. C. Lee, "Fuzzy logic in control systems: fuzzy logic controller II," IEEE Trans. On Systems, Man and Cybernetics, vol. 20, no. 2, pp. 419-435, 1990. doi:10.1109/21.52552

[49] W. V. Leekwijck, E. K. Etienne, "Defuzzification: criteria and classification," J. of Fuzzy sets and systems, vol. 108, no. 2, pp. 159-178, 1999. doi:10.1016/S0165-0114(97)00337-0

[50] I. H. Altas, A. M. Sharaf, "A generalized direct approach for designing fuzzy logic controllers in Matlab/Simulink GUI environment," Int. J. of Inf. Technology and Intelligent Computing, vol. 1, no. 4, pp. 1-27, 2007.

[51] W. C. Schultz, V. C. Rideout, "Control system performance measures: Past, present and future," IRE Trans. on Automatic Control, vol. 1, pp. 22-35, 1961. doi:10.1109/TAC.1961.6429306

[52] J. Kennedy, R. Eberhart, "A new optimizer using particle swarm theory", in Proc. of the sixth international symposium on micro machine and human science, vol. 1, pp. 39-43, 1995. doi:10.1109/MHS.1995.494215